MICROTUBULE SURFACE LATTICE AND SUBUNIT

STRUCTURE AND OBSERVATIONS ON REASSEMBLY

HAROLD P. ERICKSON

From the Department of Anatomy, Duke University Medical Center,
Durham, North Carolina 27710

ABSTRACT

Neuronal microtubules have been reassembled from brain tissue homogenates and purified. In reassembly from purified preparations, one of the first structures formed was a flat sheet, consisting of up to 13 longitudinal filaments, which was identified as an incomplete microtubule wall. Electron micrographs of these flat sheets and intact microtubules were analyzed by optical diffraction, and the surface lattice on which the subunits are arranged was determined to be a 13 filament, 3-start helix. A similar, and probably identical, lattice was found for outer-doublet microtubules. Finally, a 2-D image of the structure and arrangement of the microtubule subunits was obtained by processing selected images with a computer filtering and averaging system. The 40×50 Å morphological subunit, which has previously been seen only as a globular particle and identified as the 55,000-dalton tubulin monomer, is seen in this higher resolution reconstructed image to be elongated, and split symmetrically by a longitudinal cleft into two lobes.

Microtubules from a wide variety of sources appear to have a common structure. In electron micrographs of embedded and sectioned material they appear as long hollow cylinders, about 250 Å in diameter. In negatively stained specimens, which show higher resolution detail, the wall of the cylinder appears to be a sheet of 13 longitudinal filaments 50 Å apart. Each filament seems to be a string of globular subunits 40 Å apart. The outer-doublet microtubules of cilia and flagella have been most extensively studied, primarily because they are sufficiently stable to allow isolation, purification, and specimen preparation. Using optical diffraction techniques, Grimstone and Klug (1966) determined the approximate arrangement of the subunits on the surface lattice of microtubules from protozoan flagella. Similar optical diffraction patterns and a similar lattice structure have been found in outer-doublet micro-

tubules from various other cilia and flagella (Chasey, 1972; and H. Erickson, unpublished observations). Microtubules of cytoplasmic origin, such as those from nerve cells and mitotic spindles, are labile structures, and it has been difficult to isolate them and prepare good specimens for electron microscopy. In micrographs that have been obtained, they appear to have a filamentous substructure similar to outer-doublet microtubules (Behnke and Zelander, 1967), but the substructure and surface lattice have not been studied in great detail.

Recently, conditions have been determined for dissociating and repolymerizing microtubules in centrifuged homogenates of brain tissue, and it was shown that negatively stained specimens could be prepared from the repolymerized microtubules (Weisenberg, 1972). The investigation reported here was undertaken mainly to make a detailed structural analysis of these neuronal

microtubules for comparison with microtubules from flagella. Initially, specimens were prepared directly from the tissue homogenate, but the micro-tubules appeared smooth or had large irregular clumps, and showed no high resolution structure. It was thought that this might be due to the large amount of extraneous protein and lipid, so a purified preparation of tubulin for repolymerization studies was developed. The purified microtubules showed nice high-resolution detail from which the lattice parameters could be measured and compared with those of outer-doublet micro-tubules. Reassembly of the microtubules in the purified preparation was followed by electron microscopy, and initial structures in the assembly were observed. One of these appeared to be an incomplete microtubule which showed the cylin-drical surface unrolled and flattened. Images of these flat sheets were processed by a computer filtering system to obtain a detailed picture of the surface lattice and the structure of the individual tubulin subunits.

MATERIALS AND METHODS

Purified Preparation of Tubulin for Microtubule Polymerization Studies

In a typical experiment, microtubules were polym-erized in porcine brain extracts as described by Borisy and Olmsted (1972) and were centrifuged for 15 min at 17,000 g in a Sorvall centrifuge (Ivan Sorvall, Inc., Newtown, Conn.). The centrifuge and rotor had been warmed to 35°C and kept at this temperature during the centrifugation. The supernate was discarded and the pellet was resus-pended in ¼ the original volume of extraction buffer. Negatively stained specimens of these resuspended microtubules were much cleaner and showed the fine structural details typical of the best specimens of outer-doublet microtubules. These specimens were used for microscopy of the intact microtubules, but for other work the preparation was purified further. The suspension was cooled in ice for 30 min to allow the microtubules to depolymerize. The preparation was then centrifuged at 60,000 g for 30 min at 2°C, and the supernate was warmed to 35°C to repolymerize the microtubules. After 30 min, the sample was again centrifuged for 15 min, 17,000 g, 35°C, to give the second microtubule pellet. This was resuspended in the same volume of buffer, cooled to 0°C for 30 min, and centrifuged for 30 min, 60,000 g, 2°C, as before. The supernate constituted the final purified preparation used for most of the growth experiment. Fractions were

analyzed by gel electrophoresis at each stage of purification. A similar procedure, in which the efficiency of assembly and the stability of the tubu-lin are apparently enhanced by the addition of glycerol, has recently been reported by Shelanski et al., (1973).

Electron Microscopy

To prepare negatively stained specimens, one drop of the sample was placed on a grid coated with a carbon film. The grid was drained with a filter paper, stained by washing with several drops of uranyl acetate, and drained dry with filter paper. Micro-graphs were taken on glass plates at 60,000 × mag-nification, with no objective aperture, and about 5,000 Å under focus to enhance phase contrast (Erickson and Klug, 1971). To prepare embedded specimens, small samples of the purified preparation were raised to 35°C to initiate growth, and the re-action was stopped at specified times by adding an equal volume of 5% glutaraldehyde in extraction buffer. The samples were centrifuged at 17,000 g for 15 min to form pellets. These were washed, post-fixed with osmium tetroxide, and embedded in araldite. Sections were cut and stained with uranyl acetate and lead citrate. Micrographs were taken close to focus, with an objective aperture.

Optical and Computer Processing of Images

Optical diffraction patterns of small areas of the micrographs were obtained with a system similar to that described by De Rosier and Klug (1972). Four images with good optical diffraction patterns were selected for processing and reconstruction by a com-puter system. This processing involved two image enhancement features: (a) filtering out nonperiodic noise, and (b) averaging the structure over all the identical subunits (unit cells) included in the pro-cessed image. Operationally, the system involved scanning an area of the micrograph with an auto-matic densitometer, and recording the image on magnetic tape as a 2-D array of optical densities. The 2-D Fourier transform of this array was then generated by computer, using the program system described by De Rosier and Moore (1970). This numerical transform gave the amplitude and phase at 256 × 256 discrete points in the diffraction pat-tern, and the diffraction spots seen in the optical transform appeared as spots (each consisting of 5-20 discrete points) of high amplitude. The filtering of nonperiodic noise could be accomplished by setting to zero all transform points except those within the microtubule diffraction spots, and then reconstruct-ing the image, a process equivalent to optical filtering. The second feature of the processing used here, aver-aging, was accomplished by averaging the discrete

transform points within each diffraction spot, thereby selecting a single amplitude and phase for each of the four or five spots. The filtered and averaged numerical image was reconstructed by generating the Fourier transform of these spots, and was converted to an optical image on a computer-linked image display device.

Justification of the reconstruction

In an analysis and reconstruction of this type, one must be concerned with the problem of distinguishing true structural detail belonging to the image from any that might be generated solely by the manipulation of the data. The validity of the filtering and reconstruction process is based on a series of arguments. In the first place, it is assumed that the structure of the microtubule surface is truly periodic. Therefore, it is quite proper to use the optical difffraction pattern to screen for the best images: those with the cleanest and sharpest diffraction patterns are assumed to have the best preservation and imaging of this periodic structure. It should then be noted that if the image were a perfect representation of the periodic structure, the diffraction pattern would show only the discrete diffraction spots at the reciprocal lattice points. The addition of noise from stain granularity, extra protein, and irregular perturbations of the subunits generates additional spots at random positions in the diffraction pattern, with only small changes in the main diffraction spots. Thus, if these off-lattice diffraction spots are filtered from the diffraction pattern, either optically or by computer, before reconstructing the image, the details of the periodic structure will not be changed (except for an overall enhancement) whereas the nonperiodic structural features (noise) will be eliminated. The additional processing feature of averaging the structure over all subunits is consistent with the assumption that we are dealing with a truly periodic structure in which all of the subunits are truly identical. The averaging procedure enhances those features in the image which are repeated in all subunits, while local variations in the image due to distortions, variable staining, noise, etc. are repressed. Thus, insofar as the original object is a periodic arrangement of identical subunits, the filtered, averaged image is the best approximation to the structure that can be reconstructed from the data in the original image.

It should be emphasized that there is actually very little manipulation of the data in the sense of imposing artificial constraints or introducing arbitrary features. The diffraction pattern, in particular the computer-generated numerical transform, is obtained directly from the electron micrograph, and the image may be reconstructed from it unchanged by a second Fourier transform. The only manipula-

tion involves filtering out the off-lattice transform points and selecting a single, average amplitude and phase for each of the main diffraction spots. This amplitude and phase thus determined is in no way arbitrary, however, but is obtained directly from the original image, and presumably represents accurately the average periodic structure in the original image. The reconstructed image is then generated directly from these points, the only further manipulation being the trivial constraint of placing the points on the model lattice.

A final verification of the reconstruction is in identifying the structural features in the original image. The background noise in these images makes the identification of individual subunits very difficult, and details within the subunits are very obscure, but occasional areas can be found which resemble the structures in Figs. 6 and 7. Probably the most significant structural feature in the reconstructed image is the symmetrical splitting of the subunits. Without localizing the individual subunits, this feature can be clearly seen in the average (by sighting down the image) as a more or less symmetrical splitting of the filaments by a thin line of stain. Finally, it should be noted that optically filtered images, in which there is negligible averaging, do show considerable variation over different areas of the image, but in the "best" areas, the structure is the same as in the computer processed images.

RESULTS AND DISCUSSION

Purity of the Reassembly Mixture

Upon gel electrophoresis in sodium dodecyl sulphate, the second microtubule pellet showed a single band of tubulin (the conditions used did not separate the α and β tubulin) plus several bands of high molecular weight, together containing about 5–15% as much Coomasie Blue stain as the tubulin band. The highest molecular weight band comigrated with the major band in a preparation of dynein from Tetrahymena cilia (the supernate of an EDTA dialysate, generously provided by Dr. J. J. Blum). Two or three other bands, each frequently resolved into a doublet, migrated between myosin (200,000 daltons) and dynein (500,000 daltons) (Linck, 1971). It should be noted that similar high molecular weight proteins were found in preparations of microtubules that were stabilized and isolated directly from tissue homogenates by quite different procedures (Kirkpatrick et al., 1970). The electrophoretic pattern of the first microtubule pellet was virtually identical, with a few additional weak contaminating bands. Rough quantitation indicated that

only about 10% of the tubulin and high molecular weight proteins were recovered in the pellet after each polymerization.

The high molecular weight proteins apparently polymerize and depolymerize with the microtubules, but it is not known if they are incorporated into the microtubule structure. Since they comprise only about 10% of the protein, they would probably not be obvious in images unless they were grouped together, say in an initiation complex at one end. No localized structural differentiation has been found so far. Alternatively, they may be unrelated to microtubule assembly, either adhering nonspecifically to the microtubules, or polymerizing as independent aggregates.

Early Structures in Polymerization

The growth of microtubules was monitored by preparing negatively stained specimens at different times after raising the temperature to 35°C. The method can give quantitative counts of microtubules (Kirkpatrick et al., 1970), but only qualitative results will be discussed here. In most experiments, growth was complete in about 10 min, and specimens prepared over the next 2 h showed a fairly constant number of microtubules several μm long. Specimens prepared from tubulin at 0°C and stained with cold uranyl acetate showed numerous ring-like structures similar to those reported by Borisy and Olmsted (1972), but larger. In my preparations the rings were normally 420 Å outside, and 290 Å inside diameter, with frequent variation of up to 10%, and closely resembled single loops of vinblastine-induced aggregates. The rings may be involved in initiation of assembly as suggested by Borisy and Olmsted (1972). Alternatively, they may be simply an aggregation form of active tubulin favored at low temperature, unrelated to assembly at 37°C. Specimens prepared after 1-5 min growth at 37°C showed short microtubules, most of them being less than 1 μm after 2 min growth. It has not yet been determined whether the subsequent growth, from 2 to 10 min, involves initiation of new microtubules or merely elongation of ones already present.

In addition to the short microtubules, a number of other structures were found in specimens prepared in the first few minutes of growth. Strands and filaments, smaller in diameter than microtubules, but with no apparent regular fine structure, were found alone and in aggregated clumps. Large membranous sheets, up to 1 μm

wide and several μm long, were often found. The long edge of these sheets was sharp and straight, but no other clear substructure could be seen. These sheets may be an alternative aggregation form of microtubule protein that disappears as the protein is incorporated into microtubules, or may be an aggregate of microtubule precursor structures. Neither the small filaments nor the large membranous sheets were found frequently after 5 min growth.

The most interesting early growth structure is a small flat sheet which seems to be an incompletely formed microtubule. Typical micrographs of these sheets are shown in Figs. 1 and 3 a. They are up to 1 μm long and 650 Å (the circumference of a microtubule) wide. Longitudinal filaments 50 Å apart are clearly distinguished and can be counted, the number of filaments varying commonly from 10 to 12. Smaller sheets with less than 10 filaments were seen frequently, but were not photographed. Sheets in which 13 filaments could be counted were only occasionally found (Fig. 3 a), and sheets with more than 13 filaments were never found. Most earlier studies have concluded that there are 12 or 13 filaments making up the microtubule wall with the clearest images indicating 13 (Warner and Satir, 1973). The present findings are consistent with this in that the frequent observation of sheets with up to 12 filaments implies that these are incomplete. Open sheets with 13 filaments are rare, presumably because they have their complete complement of filaments and quickly form the intact cylinder.

Even at very early times of growth (1-2 min), only a small fraction of the microtubules appeared as flattened open sheets; most of them appeared to be short intact microtubules. However, open sheets that had collapsed on the grid and folded over could not be distinguished from intact microtubules. To investigate this further and to confirm that the incomplete microtubules were not a disintegration artifact produced by the negative stain, a growth experiment was followed by fixing and embedding specimens at various times after growth was started. After 20 min growth, only normal microtubules—i.e., hollow cylinders—were found (Fig. 2 a). At early times, many curved sheets not forming a complete cylinder were found (Fig. 2 b). In a rough count, the percentage of incomplete microtubules, i.e. those which were not closed cylinders, was: 50% at 1 min; 20% at 2 min; and 5% at 4 min. The results are thus con-
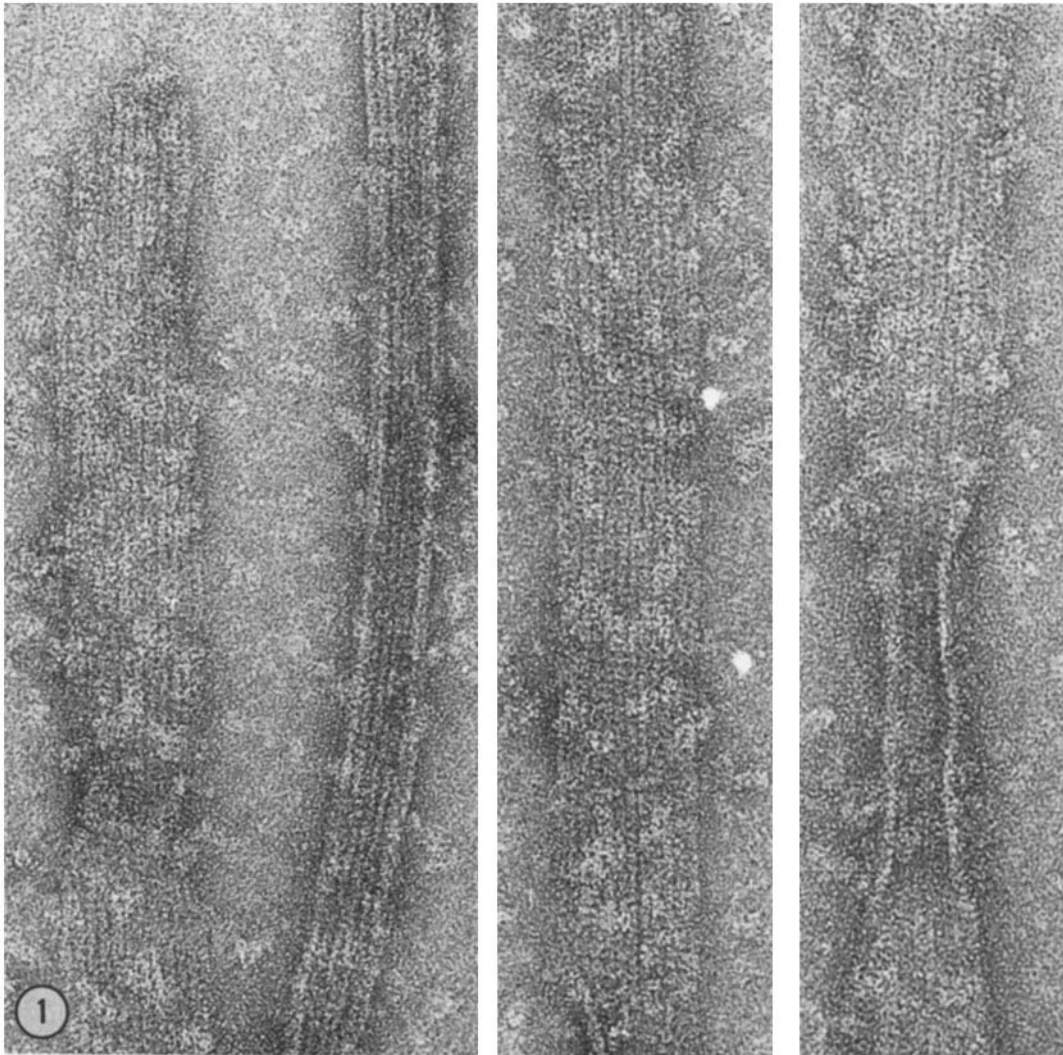
FIGURE 1 Three examples of the flattened incomplete microtubule walls from specimens prepared after 2 min at 37°C. The field at the left shows an apparently intact microtubule adjacent to the flat sheet. The sheet on the right shows the tendency to curl. The filaments may be counted most easily, and the longitudinal splitting of the filaments seen, by sighting down the images at a glancing angle. These micrographs were all taken without an objective aperture at about 5000 Å underfocus, to give optimal phase contrast enhancement (Erickson and Klug, 1971). In spite of the apparent noise, granularity, and low contrast, these images are typical of those that gave good optical diffraction patterns, and thus represent the best preservation of the periodic structural detail.

sistent with the observations on negatively stained specimens, suggesting that the incomplete open sheets are an early growth form and perhaps a precursor to the intact microtubule. Similar incomplete microtubules have been observed in vivo during polymerization of microtubules in blood platelets (Behnke, 1967). The occurrence of incomplete microtubules is greatly enhanced when

assembly is done in the presence of glycerol (Shelanski et al., 1973).

These results suggest that microtubule assembly begins with a single filament or a small aggregate of filaments. Polymerization continues primarily by elongation of existing filaments, with a slower addition of new filaments to the side of the sheet. After the full complement of 13 filaments has been
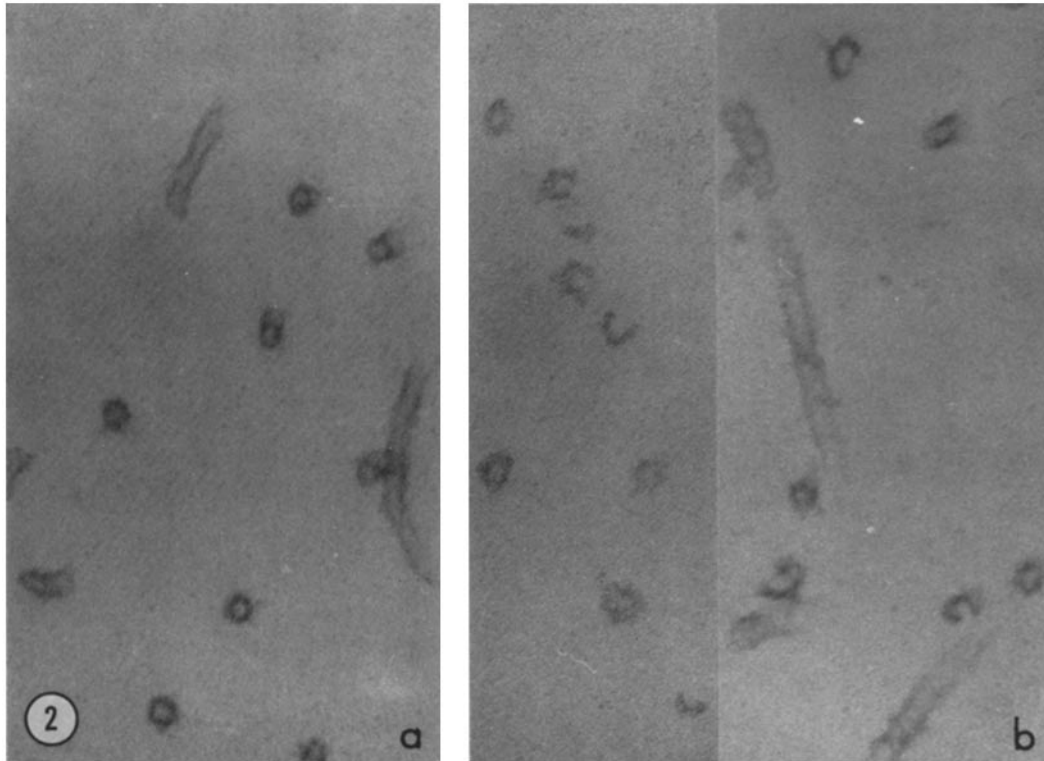
FIGURE 2 Embedded and sectioned microtubules. (a) Sample prepared after 10 min growth. Typical round hollow microtubules are seen in longitudinal and cross section. (b) Sample prepared after 1 min growth. Many of the microtubules appear in cross section as curved sheets, not complete cylinders.

added to the curved sheet, the edges meet and form bonds to make the intact cylindrical microtubule. Growth then continues by elongation. It should be noted that assembly by this mechanism could be a simple self-assembly of the tubulin subunits, not requiring a preformed circular initiator complex. However, the question of very early assembly forms and possible initiation complexes, and the role of the high molecular weight proteins in initiation and assembly needs further study.

Surface Lattice Determined from Flat Sheets and Intact Microtubules

The flattened sheet of an incompletely formed microtubule presents a simple picture of the surface lattice, equivalent to a radial projection if there are not serious distortions produced by the flattening. The most obvious lattice feature is the parallel array of longitudinal filaments. In addition to these, fainter oblique striations with a

periodicity of 40 Å and making an angle of about 10° with the horizontal can be seen in the images. This periodicity corresponds to the spacing of subunits along the filaments, with a slight staggering of adjacent filaments giving the oblique angle. When the sheet is folded around to make the cylindrical tubule, the oblique line of subunits will join up to form a helix. The surface lattice of this structure is essentially that proposed by Grimstone and Klug (1966) from images and optical diffraction patterns of intact microtubles.

The optical diffraction pattern allows the most precise measurement of the lattice parameters. The most common pattern is that shown in Fig. 3 c and diagrammed schematically in Fig. 4. There are two prominent spots on the 40-Å layer line and two orders of a 50-Å equatorial spot. These spacings and the angle were measured from the diffraction patterns of 24 images, after selecting areas that gave the sharpest and cleanest patterns. The longitudinal spacing (between subunits along the filament) was 39.8 ± 0.5 Å; the equatorial

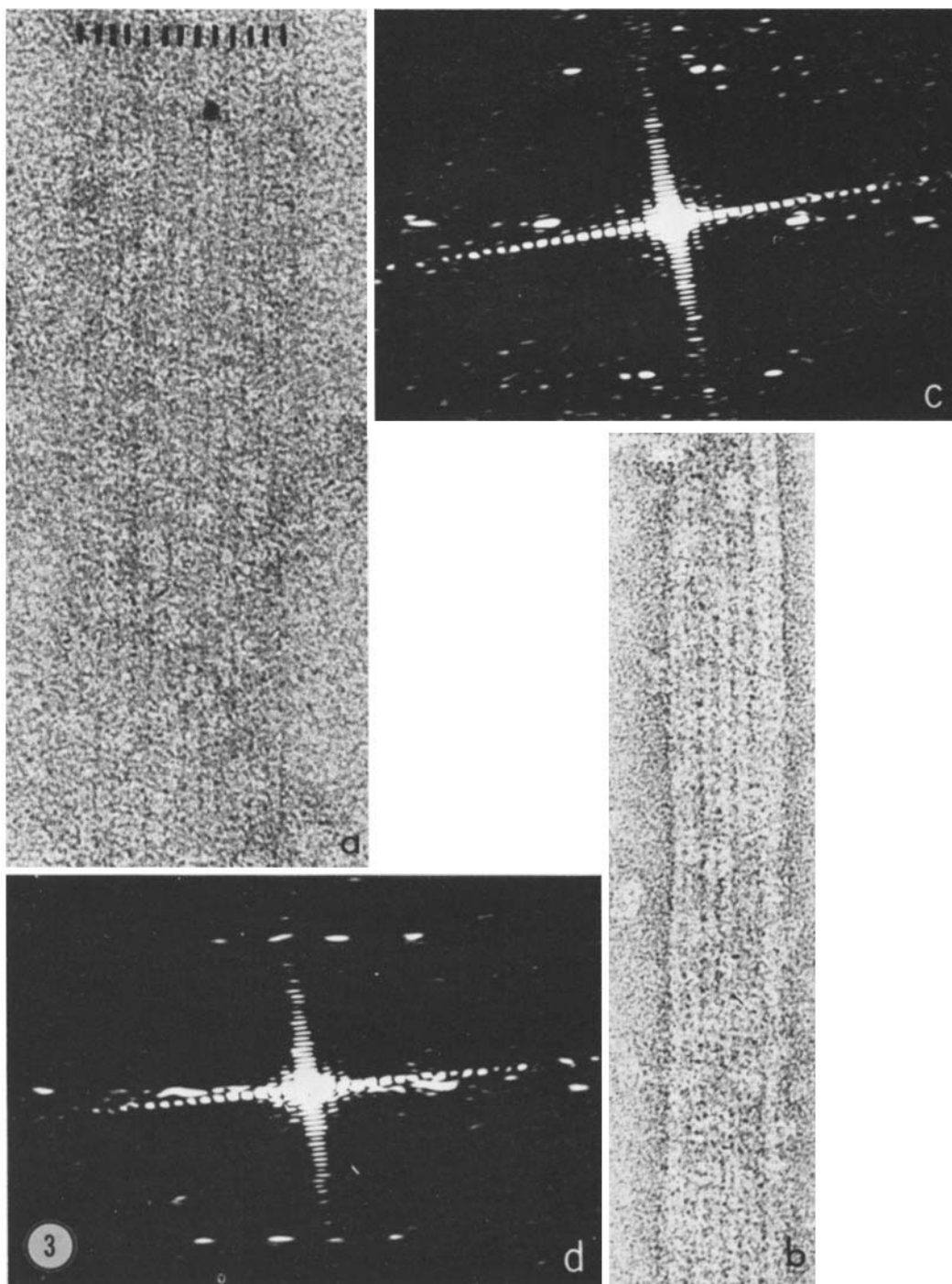FIGURE 3   Image of a flat opened sheet (a) and an intact microtubule (b) and their optical diffraction patterns. The specimen for (a) was prepared from the purified microtubule growth mixture 2 min after warming to 35°C. Fine detail in this image is largely obscured by the granular background, but the diffraction pattern (c) shows that the periodic structure is well preserved. Thirteen filaments can be counted by sighting down the sheet, and a thin line of stain may be seen running down the middle of each filament. The optical diffraction pattern of this image (c) is the typical pattern from the flat sheets. It shows two orders of the 51-Å equatorial spot and two spots on the 40-Å layer line. The intact microtubule in (b) was prepared from the microtubule pellet resuspended at 35°C. The optical diffraction pattern from the image (d) is the typical pattern from intact microtubules, with four horizontally elongated spots on the 40-Å layer line. Two of these are from the side next to the carbon film, and are essentially the same as in the pattern of the flat sheets. The other two come from the other side of the microtubule and therefore appear with the opposite hand. All images are printed to have the same hand as the image on the screen of the microscope, and are thus a view of the specimen through the carbon film. Protein is white, and stain is black.

spacing (between filaments) was 50.2 ± 1.1 Å; and the angle of the striations (the pitch angle of the helix) was 9.8 ± 1.1°. The error limits are the standard deviation, and reflect variations in the different images, rather than errors of measurement.

From these parameters, the average surface lattice of the flat sheets can be constructed. This lattice is further constrained, however, by the requirement that it must be rolled up to make a cylinder on which the subunits are arranged with helical symmetry. Thus, the oblique line of subunits must fold around to form a continuous helical line without any discontinuity at the seam. In addition, one wants to introduce little or no twist in the longitudinal filaments, since these are always observed to be straight and parallel to the axis in intact microtubules (Grimstone and Klug, 1966).

From the average lattice parameters given above, the vertical staggering of the subunits from one filament to the next is 50.2 Å × tan 9.8° = 8.68 Å. Assuming that there are 13 filaments in the sheet, rolled up into a cylinder so that the first and thirteenth filaments are adjacent, the total rise of the line of subunits in one circuit around the cylinder is 113 Å. This is very close to 3 times the 40-Å vertical spacing between subunits, so that only a small distortion will be needed to increase the pitch to 120 Å and remove the discontinuity between the first and thirteenth filaments. In fact, the average pitch determined from the 24 independent images was 113 ± 11 Å, so a true pitch of 120 Å is within the error of this determination. The microtubule structure is thus described as a 3-start helix, with each of the 3 basic helices having a pitch of 120 Å and 13 subunits per turn.

The data cannot be used to determine the number of filaments, since models with 12, 13, or 14 filaments would all give a pitch close enough to the 120 Å required for the 3 start helix. The 13 filament model is preferred for reasons given above. The data do, however, seem to limit the model to a 3-start helix. A 2-start helix would require a pitch of 80 Å, and a 4-start helix, a pitch of 160 Å. These are well outside the error limits of the determination, and are even outside the extreme values of pitch found in individual images, namely, 88 Å and 150 Å.

The typical diffraction pattern of an intact microtubule (Fig. 3 b) has one or sometimes two orders of the 50-Å equatorial spot, and has four spots on the 40-Å layer line. The pattern can be indexed as the superimposition of two of the flat sheet lattices with some notable differences. Diffraction spots from the flat sheets are relatively sharp points, whereas those from intact tubules are elongated horizontally because of the smaller width of the diffracting image and the curvature of the lattice surface. The 40-Å vertical spacing is a constant feature, but the 50-Å spacing between filaments is more variable, and is usually different for the two sides of a microtubule. Normally, the lattice from one side shows a filament spacing close to 50 Å, while the other side gives a value of 35–45 Å, indicating that this side has partially collapsed, squeezing the filaments together. This phenomenon has been noted and discussed by Moody (1967).

Because of the broadening of the spots, the curvature of the surface, and the distortion of the lattice, measurements from the diffraction patterns of intact tubules are more variable and ambiguous than those from the flat sheets. Diffraction patterns of nine images of intact microtubules were measured and the lattice parameters were determined from each side. Although one side usually showed reduced filament spacing, this would be compensated for by an increased pitch angle, since the structural integrity and continuity of the surface lattice seems to be maintained. Consequently, the pitch calculated from the parameters ($pitch = 13 \times d$ tan θ, where d is the filament spacing and θ is the pitch angle) should not be greatly affected by the distortion. The 18 measurements gave a value for the pitch of 127 ± 17 Å. This is quite close to the 120-Å pitch of the 3-start helix, and is confirming evidence that this is the structure of the surface lattice in the intact microtubule.

The absolute hand of the helix has been determined to be left-handed by two observations. First, it is found that all of the flat sheets are skewed in the same way—i.e., the oblique lines run to the left and up when viewing the micrograph emulsion up. (All images are printed to give this view.) It is reasonable to assume that the outside surface of the microtubule sheet, which is curved to make an incomplete cylindrical wall, contacts the carbon film and the sheet spreads open and flattens in this orientation. Since the specimen is then inverted in the microscope, the image is one looking at the sheet through the

carbon film, and is therefore a view of the microtubule surface from the outside. The helix is therefore seen to be left-handed. The second observation is from the diffraction pattern of intact microtubules, in which the lattice from one side is observed to have flattened and shrunk. This lattice is always found to be the one with the opposite orientation to the lattice of the flat sheets, implying that it is the side away from the carbon film. Moody (1967) argues that the upper surface is normally collapsed, so this observation may be taken either as confirmation that the helix is left-handed, or as confirmation of Moody's argument.

Conflicting Models for the Surface Lattice

Two different models for the microtubule lattice structure have been proposed recently for outer doublet microtubules from cilia and flagella. Chasey (1972) has attempted to determine the lattice by measuring the pitch angle from optical diffraction patterns of intact microtubules. He found an average value for the angle of 15°, and assuming a filament spacing of 50 Å, concluded that the microtubule must be a 4-start helix. I have done similar measurements on images of sea urchin sperm microtubules (prepared as described by Stephens [1970] and negatively stained with uranyl acetate) in which the pitch angle and filament spacing were measured independently for each side, and the pitch calculated as above. The difference between the two sides was much more pronounced than in images of brain microtubules. The side away from the carbon film (the one which is noticeably collapsed and flattened) gave a pitch of 132 ± 14 Å, while the side next to the carbon film (which preserves the 50-Å filament spacing and also presumably the curvature of the surface much better [Moody, 1967]) gave a value of 164 ± 15 Å (10 measurements each). The first value agrees best with the 3-start helix, while the second value implies a 4-start helix. Since these measurements and calculations are based on the assumption of a flat lattice, it is tempting to accept the values from the flattened and collapsed surface, and to suggest that the higher values obtained for the better preserved curved surface are complicated by structural features in the third (radial) direction. Further evidence that the outer-doublet and neuronal microtubules have the same lattice structure is provided by experiments in which fragments of outer-doublet microtubules have been used as initiators for the growth of brain microtubules, the polymerized brain microtubules growing as extensions of the outer-doublet fragments (Borisy, private communication). Continuity of the hybrid microtubule would require that they have identical lattices.

A different lattice structure has been proposed by Cohen et al. (1971) on the basis of X-ray diffraction pictures of outer-doublet microtubules from sea urchin sperm. Their model is characterized by a basic helix about twice as steep as the one proposed here, in which the subunits on adjacent filaments are staggered by 20 Å, or about half the 40-Å longitudinal subunit repeat. Their microtubule lattice would be a 6-start helix, instead of the 3-start helix found by electron microscopy. This model was based on the observation of fairly wide angle off-meridional diffraction peaks on the 40-Å layer line and near meridional peaks on the 20-Å layer line. It is difficult to reconcile this X-ray diffraction data with the lattice seen in electron microscope images. Cohen et al. (1971) suggest that their model should be closer to the native structure since the X-ray diffraction patterns on which it is based were obtained from hydrated specimens. They suggest that the structure seen in negatively stained electron microscope images may be disrupted and rearranged when the microtubules are stained and dried down on the grid. In support of this, they present an X-ray pattern of an air-dried microtubule fiber, which has a single strong meridional spot on the 40-Å layer line. This is interpreted as indicating disruption of the lateral coherence of the surface lattice, with the structure diffracting simply as a linear array of protein subunits. However, this description cannot apply to the negatively stained microtubules, or open sheets, since these have a high degree of order both longitudinally and laterally. The suggestion that the lattice may undergo a rearrangement under the influence of the uranyl acetate and drying also seems implausible for the following reasons. The microtubules in the negatively stained specimens are almost certainly intact: if they were not, open sheets and fragments, like those in specimens of incomplete or disrupted microtubules, should be found frequently. A lattice rearrangement would thus require breaking the lateral bonds between two filaments, distorting the lattice to halve the pitch angle, and rejoining the free edges to form the intact tubules seen in the microscope. In addition,

it is important to note that the 50-Å filament spacing and the 40-Å subunit spacing are very accurately preserved in the electron microscope specimens, whereas a drastic rearrangement of the lattice might be expected to distort these parameters significantly.

The negative staining technique has not before been shown to produce an artifactual image. Although disruption of structures by negative stain is commonly observed (e.g., microtubules stained with phosphotungstic acid) whenever well-preserved images of structures such as viruses and muscle proteins have been compared with X-ray diffraction data, they are consistent. (Negatively stained crystals of catalase were observed by Longley [1967] to be quite different in structure from the large hydrated crystals observed by X-ray diffraction or by electron microscopy of embedded specimens. Recent experiments [unreported observations of the author] have indicated that the thin flat crystals seen in negatively stained specimens are a completely different crystal form, which does not involve a rearrangement of the structure upon drying in the stain.) In the case of the microtubule studies, as in most others, it must be realized that the electron microscope gives a direct image of the lattice, whereas with X-ray diffraction the lattice must be deduced indirectly from a small set of rather diffuse diffraction spots. In the absence of evidence that the electron microscope image is artifactual, it seems most reasonable to try to resolve the apparent inconsistency by looking for alternative interpretations of the X-ray diffraction data.

The microtubules and sheets in the negatively stained specimens are either partially or completely flattened, whereas the microtubules in the fiber specimens for X-ray work are presumably undistorted. The inconsistency of the two observations may involve unknown aspects of the 3-D structure, which is different in the two types of specimens. The X-ray data consist essentially of three diffraction spots, two of which are consistent with the model proposed here: the 50-Å equatorial is identical in the two models, and the near meridional on the 20-Å layer line will fit with the present model if account is taken of the considerable lateral blurring of the spot in the X-ray pattern. The off-meridional spot on the 40-Å layer line presents the only problem. To fit with the present model, this spot would have

to be identified with either the (0, 1) spot or the ($\bar{1}$, 1) spot in Fig. 4, which would correspond to Bessel functions J_3 or $J_{\overline{10}}$ in the diffraction pattern from the intact microtubules. If the spot does correspond to the maximum of the J_3 Bessel function, the diffracting structures giving rise to it must be very far on the inside of the microtubule, at an average radius of 45 Å. If the spot corresponds to the maximum of $J_{\overline{10}}$, the diffracting structures must be on the outside surface of the microtubule, at an average radius of 135 Å. Then one must also assume that the maximum of J_3 is, for some reason, much weaker in the X-ray pattern than in the patterns from electron microscope images and is obscured in the blurred intensity near the meridian on the 40-Å layer line. In either case, the equatorial spacing would correspond to the maximum of J_{13}, which must then derive from structure at a radius of 100Å. Thus, the X-ray diffraction data might be reconciled with the lattice seen by electron microscopy if the structural details giving rise to the scattering on the equator and on the 40-Å layer line are at different radii in the microtubule. Of course, this possibility is completely speculative at present, but it is hoped that 3-D information from elec-
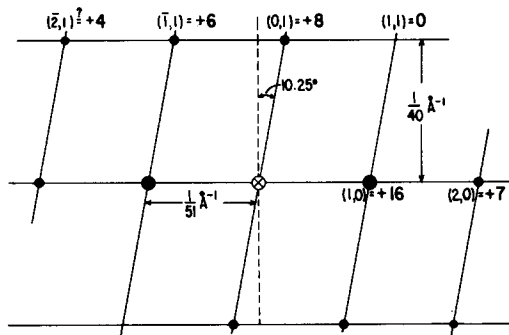

FIGURE 4 The model diffraction pattern of the flattened microtubule sheet. The lattice parameters were adjusted slightly from the average to agree exactly with the 13 filament, 3-start helix proposed for the intact microtubule. The indexing of the spots on a 2-D lattice is indicated in the parentheses, and the amplitudes of the spots determined from computer transforms of four images is given in bolder type. With the proper choice of origin for the calculation of the transform, the phase angles of all the spots were zero degrees, and this is indicated by the plus sign before each amplitude. The spot at position ($\bar{2}$, 1) was observed only occasionally. Figs. 5 and 6 show the image reconstructed without this spot, and Fig. 7 is that obtained when it is included.

tron microscopy of intact microtubules and tilted specimens of flat sheets will clarify the situation in the future.

Filtering and Reconstruction

In the original micrographs of the flat sheets, the longitudinal filaments can be distinguished easily, the oblique striations are more difficult to see, and finer substructure of subunits making up the lattice is much more obscure. One higher resolution detail that can be seen by sighting down the sheet is a thin line of stain running down the middle of each filament. This splitting of the filaments can be seen also in fragments of disintegrating sperm tail microtubules and in optically filtered images of intact sperm tails (unpublished observations) and has also been observed and described recently as two helically wound subfilaments making up each longitudinal filament (Warner and Meza, 1972). The clearest images of microtubules were obtained from specimens prepared immediately after resuspending the microtubule pellet. Specimens prepared from the reassembly mixture, from which the images of the flat sheet were obtained, show less detail, presumably because the large amount of unpolymerized tubulin is contributing to the background noise and obscuring detail in the images. Nevertheless, the optical diffraction patterns show diffraction spots out to 25-Å resolution, so periodic structural detail to this resolution is present in the images.

The computer processing system was used to reconstruct a filtered and averaged image that shows the high resolution structure. Optical filtering was also used and gave similar results, and only the final image from the computer reconstruction is presented here. To obtain this, four images were processed by generating the numerical transform, as described in Materials and Methods, and the average amplitude and phase of each of the diffraction spots was determined. The amplitudes of the spots were somewhat variable, depending on the image and the focus-dependent phase contrast (Erickson and Klug, 1971), but the reconstructed image was relatively independent of these variations. The phase angles of the spots were identical in all four images. With the proper choice of origin, they were all within 15° of zero so the phases could be designated by assigning a plus sign to each amplitude. (The implication of the zero degree phase angle is that the four cosine waves corresponding to the diffrac-

tion spots all have their origin, which is their peak density, at the same place, namely the black spots of stain between filaments in Fig. 6. The zero degree phase angle of the [1, 0] and [0, 1] spots is arbitrary in that it defines the choice of origin. The zero degree phase angle of the other two spots is related to the symmetrical splitting of the subunits, as may be seen by tracing sets of lines corresponding to the peaks of the cosine waves over the reconstructed image in Fig. 6.) The model transform giving the average amplitude of the diffraction spots is shown in Fig. 4. The processed image (Figs. 5 and 6) was reconstructed by generating the Fourier transform of the four spots in this model transform. This image shows the arrangement of the subunits on the model surface lattice and also shows higher resolution structural details of the individual subunits.

Several features of the structure are worth noting. In earlier studies, the repeating subunit has been described as a 40 × 50 Å globular particle, usually identified as the 55,000-dalton tubulin monomer. In the higher resolution processed image presented here, this subunit is seen to be elongated and skewed at a 40° angle from the horizontal. The most interesting feature is the longitudinal cleft, which divides each subunit into two apparently identical halves. Since this subunit appears morphologically to be a dimer, it would be tempting to identify it as the 110,000-dalton tubulin dimer, which is the stable chemical subunit. However, it is fairly clear that only a single 55,000-dalton monomer can fit in this space (Shelanski and Taylor, 1968), so the cleft seems to be within the monomer. The division of the subunit into two lobes might be understood in view of the fact that several large proteins have been found to be similarly divided, and it may represent a common structural feature of proteins larger than 20,000 daltons (see Matthews et al., 1972). It should be noted that the absolute size of the subunits as seen in the reconstructed image is influenced by a number of factors, especially by the limited resolution of the reconstruction, and does not correspond to the actual size of the protein molecules. Only the features of shape— elongation, skew, and the longitudinal cleft—are reliably represented. In addition, it must be emphasized that this is a 2-D projection from one angle of view, and it is likely that the two lobes of the subunit are at different heights.

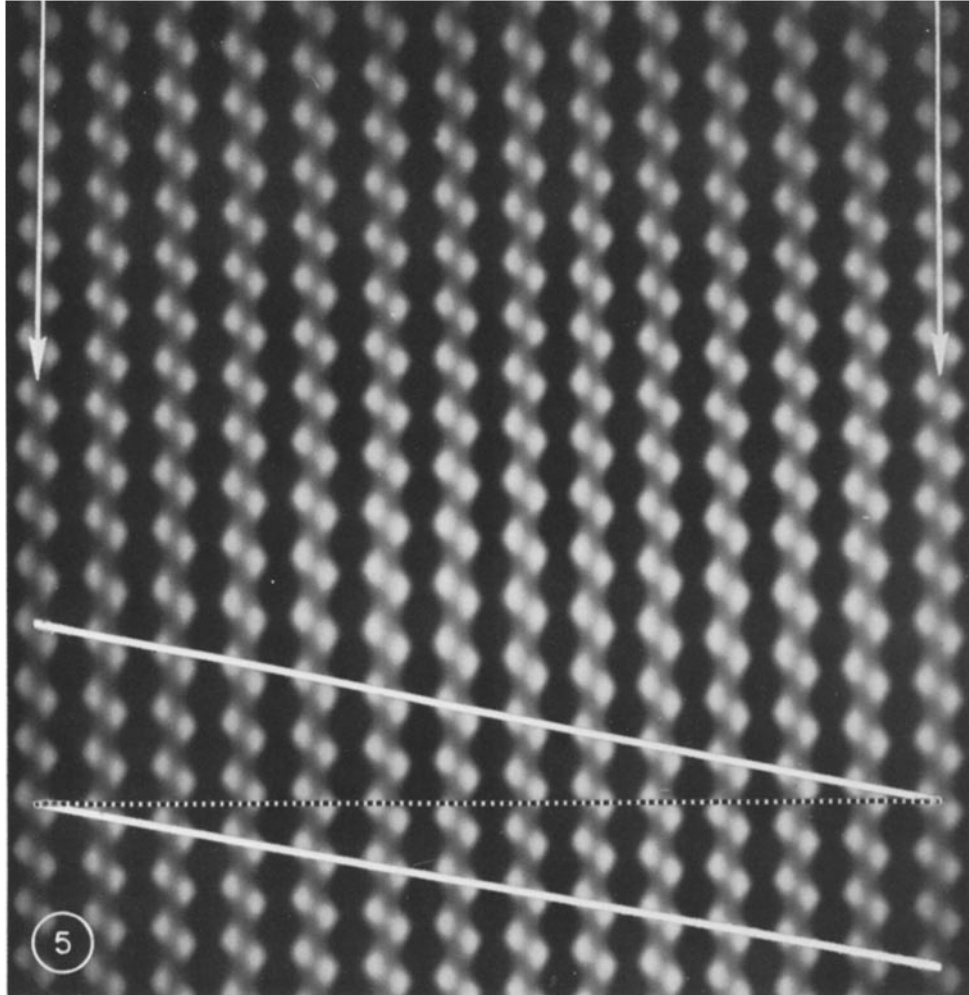The only significant deviation from this struc-

FIGURE 5 The computer reconstructed image of the flattened microtubule sheet. This image is the Fourier transform of the model transform diagrammed in Fig. 4, using only the four spots in the typical diffraction pattern ($[\bar{2}, 1] = 0$). The direction of view is from the outside to the inside of the microtubule, and the image is printed so that protein is white, stain is black. The sheet may be rolled up to make a cylinder, superimposing the first and fourteenth filaments (arrows), without bending or distorting the longitudinal filaments. The oblique line represents the basic helix of the 3-start helical lattice.

ture that was found in the experimental work was the occasional observation of a diffraction spot at the $(\bar{2}, 1)$ position. When this spot was included in the reconstruction the image seen in Fig. 7 was obtained. The most obvious effect of including this spot is the extra density added to the middle of the subunit, obscuring the cleft that runs completely through the subunit in Fig. 6. The division of the subunit into two lobes is still indicated by the indentation at the top and the bottom, and by the connections between subunits which are emphasized in this reconstruction. It is

notable that these connections are between like sides of adjacent subunits, i.e., all the left lobes are connected longitudinally, as are the right lobes, and the only obvious connection between the right and left sides is across a single subunit. The splitting of the filaments now seems to be due to the vertical connections between subunits, one connection on each side of the filament. Since the $(\bar{2}, 1)$ spot that generates these different structural features was observed only rarely, it is felt that Fig. 6 may be the better representation of the structure. The images showing this extra detail

might have come from slightly tilted areas of the specimen, in which case Fig. 7 would represent a projection of the subunit structure from a different angle of view. Alternatively, the detail may be real, but only rarely preserved by some particular condition of stain. It should be emphasized, however, that in spite of the apparent differences in the two images, the main structural features—
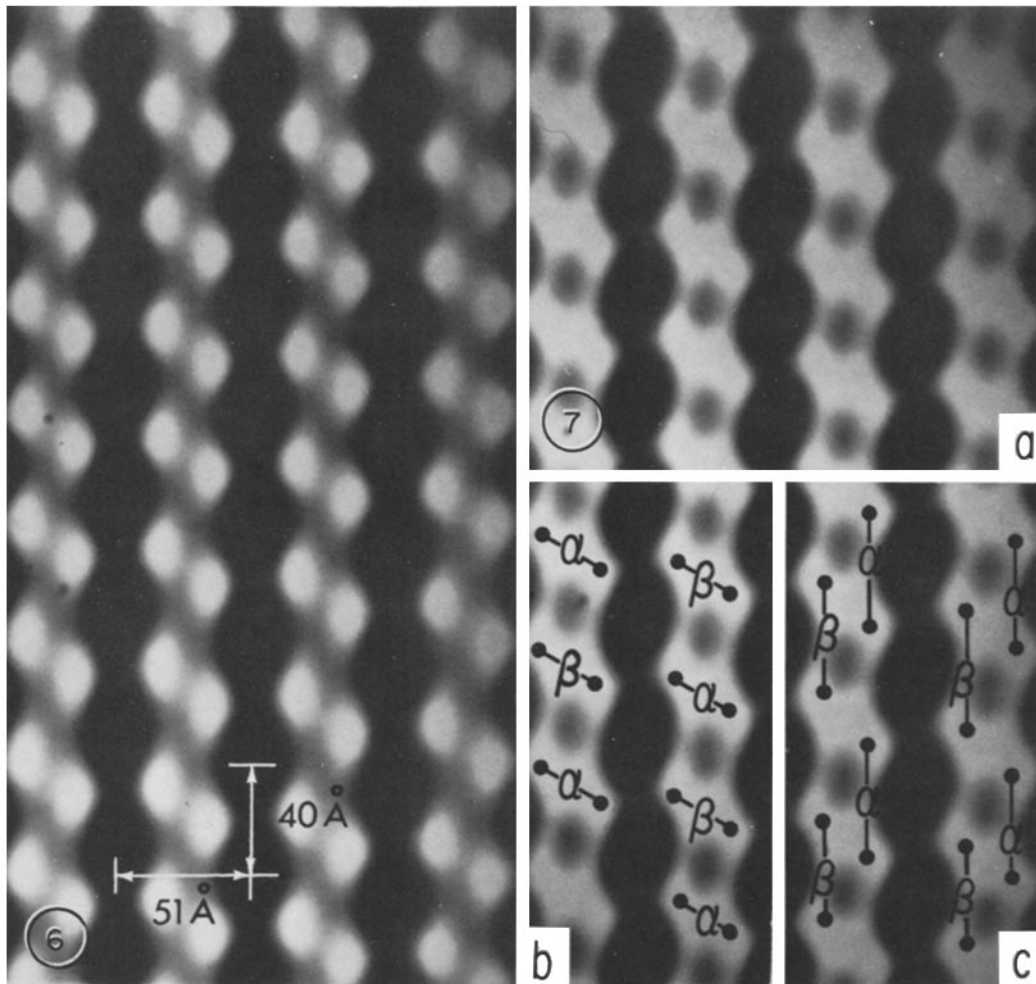

FIGURE 6 A higher magnification view of the image reconstructed as in Fig. 5, with $(\bar{2}, 1) = 0$. The repeating morphological subunit in the 40×51 Å unit cell corresponds in size to the 55,000-dalton tubulin monomer (Shelanski and Taylor, 1968). It appears in this 2-D projection to be elongated, skewed about 40° from the horizontal axis, and split into two equal parts by a longitudinal cleft. The apparent small size of the protein subunits, and the large spaces (stain) between them is artifactual, since the absolute size of the repeating structures is not reliably represented in this reconstruction.

FIGURE 7 Image reconstructed with the addition of the diffraction spot at position $(\bar{2}, 1)$. The cleft splitting each subunit is partly obscured, and connections between adjacent subunits along a strand are more obvious than in Fig. 5. The extra diffraction spot that generates these changes occurs infrequently in the images of the flattened sheets and may be due to a small tilt of the specimen.

Two possibilities for the identification of the tubulin monomer, and for the arrangement of α and β type tubulins are given in (b) and (c). The most obvious identification is shown in (b), where each of the morphological repeating subunits is identified as a tubulin monomer. The alternating arrangement of α and β types indicated is the only one consistent with the 13 filament, 3-start helix. Alternatively, the structure might be drawn with the monomers arranged longitudinally. One possible arrangement of this type is indicated in (c).

the elongation, tilt, and symmetrical splitting or division of the subunits—are similar in each case.

It is now known that there are two slightly different types of tubulin monomer. These two types, referred to here as "α" and "β", occur in equal amounts in brain microtubules (and in other microtubules examined) and it seems likely that the microtubule is constructed from heterodimers (Bryan and Wilson, 1971; Olmsted et al., 1971). In their previous studies of microtubule structure by optical diffraction, Grimstone and Klug (1966) observed a more or less well-developed 80-Å layer line, indicating a morphological difference or staggered displacement of alternate subunits. It has been attractive to think of this 80-Å periodicity as reflecting the pairing of tubulin monomers to form dimers and perhaps also showing a morphological difference between the two types. However, in the present study, spots were never found, or were at best diffuse and weakly developed, on the 80-Å layer line from either the flat sheets or intact microtubules. The same absence of an 80-Å layer line was found in the survey of sea urchin sperm microtubules and in an earlier study of microtubules from *Tetrahymena* cilia (unpublished observations). In these latter cases, the specimens were made from microtubules that had been purified by dialyzing against EDTA and washing. The specimens of Grimstone and Klug showing the 80-Å layer line, and those used by Chasey (1972) in which a weakly developed, but fairly consistent 80-Å layer line was found, were prepared from intact organisms or cilia. The microtubules might be simply in a better state of preservation in these specimens, as suggested by Grimstone and Klug (1966), but it is also possible that the structure giving the 80-Å layer line is extraneous to the microtubule proper and is easily stripped off in the purification and staining. Microtubules from the sperm of flatworms, which show a strikingly well-preserved 80-Å periodicity (Burton, 1966), are being investigated in the hope of answering some of these questions.

In any case, since no consistent 80-Å data were found in these images, none was included in the reconstruction. All of the subunits in the reconstructed image are thus identical in structure and position. Nevertheless, the question of the identity of the α and β tubulin monomers in the structure is interesting and can be indicated schematically. Fig. 7 shows two different possibilities. The most obvious is to identify each of the repeating mor-

phological subunits as tubulin monomers, and label them schematically α and β. The 13 filament, 3-start helix proposed here imposes constraints on the arrangement of the two types of subunits. There is, in fact, only one arrangement that preserves helical symmetry. This is indicated in Fig. 7 *b*, in which the subunits alternate both along the filament and around the basic helix. Models which do not preserve symmetry (Witman et al., 1972) are less attractive, especially for cytoplasmic microtubules which show no obvious departure from symmetry. A different identification of the subunits is indicated in Fig. 7 *c*. Here, the monomer is again interpreted as divided into two lobes, but is now drawn running longitudinally, with one lobe in each of two adjacent 40-Å morphological subunits, and the α and β types on opposite sides of the filament. Numerous variations on this type arrangement can be designed that are consistent with helical symmetry. The longitudinal arrangement of the monomers is similar to a model proposed by Warner ([1972] and personal communication). However, the globular appearance of the subunit lobes and the connections between lobes on each side of the filament, which are apparent in these reconstructed images, are quite different from the helical strands proposed in that model. Each of the two types of arrangements indicated in Fig. 7 has certain attractive features, but until structural information about subunit differences is included in the model, the identification of the tubulin monomers must be considered only schematic.

Note Added in Proof: The determination of helical parameters and the indexing of the diffraction pattern has been determined for intact outer-doublet microtubules by rather different criteria than those used here (Amos, L. A., and A. Klug. 1973. *J. Cell*

Sci. In press.). The same structure was deduced, giving Bessel functions of order 3 and 10 on the 40-Å layer line. An 80-Å layer line, with Bessel functions of order 5 and 8, was observed in this study and was related to a radial staggering of alternate subunits.

REFERENCES

BEHNKE, O. 1967. Incomplete microtubules observed in mammalian blood platelets during microtubule polymerization. *J. Cell Biol.* **34**:697–701.

BEHNKE, O., and T. ZELANDER. 1967. Filamentous substructure of microtubules of the marginal bundle of mammalian blood platelets. *J. Ultrastruct. Res.* **19**:147–165.

BORISY, G., and J. OLMSTED. 1972. Nucleated assembly of microtubules in porcine brain extracts. *Science (Wash. D.C.).* **177**:1196–1197.

BRYAN, J., and L. WILSON. 1971. Are cytoplasmic microtubules heteropolymers? *Proc. Natl. Acad. Sci. U.S.A.* **68**:1762–1766.

BURTON, P. R. 1966. A comparative electron microscopic study of cytoplasmic microtubules and axial unit tubules in a spermatozoon and a protozoan. *J. Morphol.* **120**:397–424.

CHASEY, D. 1972. Subunit arrangement in ciliary microtubules in *Tetrahymena pyriformis*. *Exp. Cell Res.* **74**:140–146.

COHEN, C., S. HARRISON, and R. STEPHENS. 1971. X-ray diffraction from microtubules. *J. Mol. Biol.* **59**:375–380.

DE ROSIER, D. J., and A. KLUG. 1972. Structure of the tubular variants of the head of bacteriophage T4 (polyheads). *J. Mol. Biol.* **65**:469–488.

DE ROSIER, D. J., and P. B. MOORE. 1970. Reconstruction of three-dimensional images from electron micrographs of structures with helical symmetry. *J. Mol. Biol.* **52**:355–369.

ERICKSON, H. P., and A. KLUG. 1971. Measurement and compensation of defocusing and aberrations by Fourier processing of electron micrographs. *Philos. Trans. R. Soc. Lond. Ser. B. Biol. Sci.* **261**:105–118.

GRIMSTONE, A. V., and A. KLUG. 1966. Observations on the substructure of flagellar fibers. *J. Cell Sci.* **1**:351–362.

KIRKPATRICK, J., L. HYAMS, V. THOMAS, and P. HOWLEY. 1970. Purification of intact microtubules from brain. *J. Cell Biol.* **47**:384–394.

LINCK, R. W. 1971. Comparative ultrastructure and biochemistry of cilia and flagella from the lamellibranch mollusc *Aequipectin irradians.* Ph.D. Thesis. Brandeis University, Boston, Mass.

LONGLEY, W. 1967. The crystal structure of bovine liver catalase: a combined study by X-ray diffraction and electron microscopy. *J. Mol. Biol.* **30**:323–327.

MATTHEWS, B. W., J. JANSONIUS, P. COLEMAN, B. SCHOENBORN, and D. DUPOURQUE. 1972. Three dimensional structure of thermolysin. *Nat. New Biol.* **238**:37.

MOODY, M. F. 1967. Structure of the sheath of bacteriophage T4. *J. Mol. Biol.* **25**:167–200. (See especially Fig. 4.)

OLMSTED, J. B., G. B. WITMAN, K. CARLSON, and J. L. ROSENBAUM. 1971. Comparison of microtubule proteins of neuroblastoma cells, brain and *Chlamydomonas* flagella. *Proc. Natl. Acad. Sci. U.S.A.* **68**:2273–2277.

SHELANSKI, M. L., F. GASKIN, and C. R. CANTOR. 1973. Microtubule assembly in the absence of added nucleotide. *Proc. Natl. Acad. Sci. U.S.A.* **70**:765–768.

SHELANSKI, M. L., and E. W. TAYLOR. 1968. Properties of the protein subunit of central-pair and outer-doublet microtubules of sea urchin flagella. *J. Cell Biol.* **38**:304–315.

STEPHENS, R. E. 1970. Thermal fractionation of outer fiber doublet microtubules into A- and B-subfiber components: A- and B-tubulin. *J. Mol. Biol.* **47**:353–363.

WARNER, F. D., and I. MEZA. 1972. Macromolecular and biochemical aspects of microtubule protofilaments. *J. Cell Biol.* **55**(2, Pt. 2):273 a. (Abstr.).

WARNER, F. D. and P. SATIR. 1973. The substructure of ciliary microtubules. *J. Cell Sci.* **12**:313–326.

WEISENBERG, R. C. 1972. Microtubule formation *in vitro* in solutions containing low calcium concentrations. *Science (Wash. D.C.).* **177**:1104–1105.

WITMAN, G. B., K. CARLSON and J. L. ROSENBAUM. 1972. *Chlamydomonas* flagella. II. The distribution of tubulins 1 and 2 in the outer doublet microtubules. *J. Cell Biol.* **54**:540–555.